Oxygen and Carbon Isotopes in Marine Carbonates: A Biogenic Climate Archive Built Upon Disequilibria

Sang Chen[1] and James M. Watkins[2]

1811-5209/25/0021-0112$2.50 DOI: 10.2138/gselements.21.2.112

Live planktonic foraminifera *Trilobatus sacculifer* from the Red Sea spreading its rhizopodia, with a ring of symbiotic dinoflagellates surrounding the $CaCO_3$ test. Image credit: Jonathan Erez.

The stable isotopic composition of marine biogenic carbonates is one of the main archives for paleoclimate reconstructions. Reading these archives accurately requires understanding of how different organisms make carbonate minerals, and how various biomineralization processes influence stable isotope fractionation. New developments in stable isotope measurements, laboratory experiments, and biomineralization modeling have progressively enabled us to disentangle the environmental and biological controls on the stable isotope proxies, and offer promise for a deeper understanding of how calcifying organisms record and respond to changes in Earth's climate and carbon cycle through geologic time.

Keywords: marine biogenic carbonates; oxygen and carbon isotopes; paleoclimate; vital effects

MARINE CALCIFYING ORGANISMS: THE PRIMARY ARCHIVE

As a water planet that hosts life, a significant proportion of Earth's climate history, from Phanerozoic to paleoseasonal timescales, is archived in calcium carbonate ($CaCO_3$) minerals built by various marine organisms. Over the last nearly seven decades, studies of the stable oxygen and carbon isotope compositions (denoted $\delta^{18}O$ and $\delta^{13}C$, respectively, which measure the relative deviations in $^{18}O/^{16}O$ and $^{13}C/^{12}C$ ratios of a sample from an international standard) of foraminifera shells in deep-sea sediments have produced an iconic record of Earth's climate history, as worlds of dramatically different climates in the past are recorded in grains of $CaCO_3$ sand made by these single-celled protists (Emiliani 1955; Zachos et al. 2001; Westerhold et al. 2020).

The benthic foraminifera record over the last 66 million years is nearly continuous, revealing trends, rhythms, and aberrations in Earth's climate, as well as a complex yet intriguing relation between climate and the carbon cycle (Fig. 1A, 1B; Zachos et al. 2001; Westerhold et al. 2020). While the benthic $\delta^{18}O$ record primarily reflects changes in deep-sea temperature and global ice volume, the $\delta^{13}C$ record reflects shifts in the distribution of carbon among different reservoirs as a result of tectonic, climate, ocean circulation, and ecological changes. A global composite of the benthic $\delta^{18}O$ record shows a long-term cooling trend over the Cenozoic, as the Earth transitioned from an ice-free Eocene hothouse to a Pleistocene icehouse with regular glaciations (Fig. 1A; Zachos et al. 2001; Westerhold et al. 2020). This transition was likely accompanied by a systematic shift in the interactions between climate and the carbon cycle, as the $\delta^{18}O$ and $\delta^{13}C$ records switch from positive correlations in warm climates to negative correlations in cold climates (Fig. 1C; Kirtland Turner 2014; Westerhold et al. 2020).

In addition to $\delta^{18}O$ and $\delta^{13}C$, advances in clumped isotope geochemistry have provided a new tool for investigating the evolution of Earth's climate system (Ghosh et al. 2006; Meckler et al. 2022). Unlike $\delta^{18}O$ and $\delta^{13}C$, which have multiple sources of variability, the clumped isotope composition of marine carbonates (denoted Δ_{47}, which measures the preferential formation of ^{13}C-^{18}O bonds in carbonate groups in the mineral relative to random distribution of the rare isotopes) is almost purely a function of temperature (Ghosh et al. 2006). The Δ_{47} record of benthic foraminifera has not only confirmed the overall Cenozoic cooling trend indicated by $\delta^{18}O$, (Fig. 1D, 1E), but has helped deconvolve changes in deep ocean temperature from changes in seawater $\delta^{18}O$ over the Cenozoic. A combination of the two records also revealed previously underappreciated factors that may affect the $\delta^{18}O$ record, including seafloor spreading rates, ocean circulation, and seawater pH (Meckler et al. 2022). Despite lower temporal resolution, the benthic Δ_{47} record also shows larger temperature variability in the early Cenozoic compared with the $\delta^{18}O$ record, suggesting a less stable climate system in a hothouse world (Meckler et al. 2022).

While foraminifera give us a nearly continuous record of climate evolution over millennial and longer timescales, other biogenic carbonates offer the advantage of interannual to sub-annual (seasonal, monthly, or even higher) temporal resolution afforded by their high growth rates, most notably coral skeletons and giant mollusk shells. For instance, the $\delta^{18}O$, $\delta^{13}C$, and Δ_{47} of shallow-water corals exhibit regular seasonal cycles (Fairbanks and Dodge 1979; Ghosh et al. 2006; Saenger et al. 2012). However, the $\delta^{18}O$ and Δ_{47} in corals do not always agree on the magnitude of temperature fluctuations (Saenger et al. 2012), while the $\delta^{13}C$ can vary with or against $\delta^{18}O$ seasonally under different circumstances (Fairbanks and Dodge 1979). It is a longstanding and ongoing challenge to unravel the fundamental mechanisms underlying these complex relationships during the formation of biogenic carbonates.

1 Shanghai Jiao University
State Key Laboratory of Submarine Geoscience
Key Laboratory of Polar Ecosystem and Climate Change, Ministry of Education
Shanghai Key Laboratory of Polar Life and Environment Sciences
School of Oceanography
Xuhui, Shanghai, China
E-mail: sang@sjtu.edu.cn

2 University of Oregon
Department of Earth Sciences
Eugene, OR 97403, USA
E-mail: watkins4@uoregon.edu

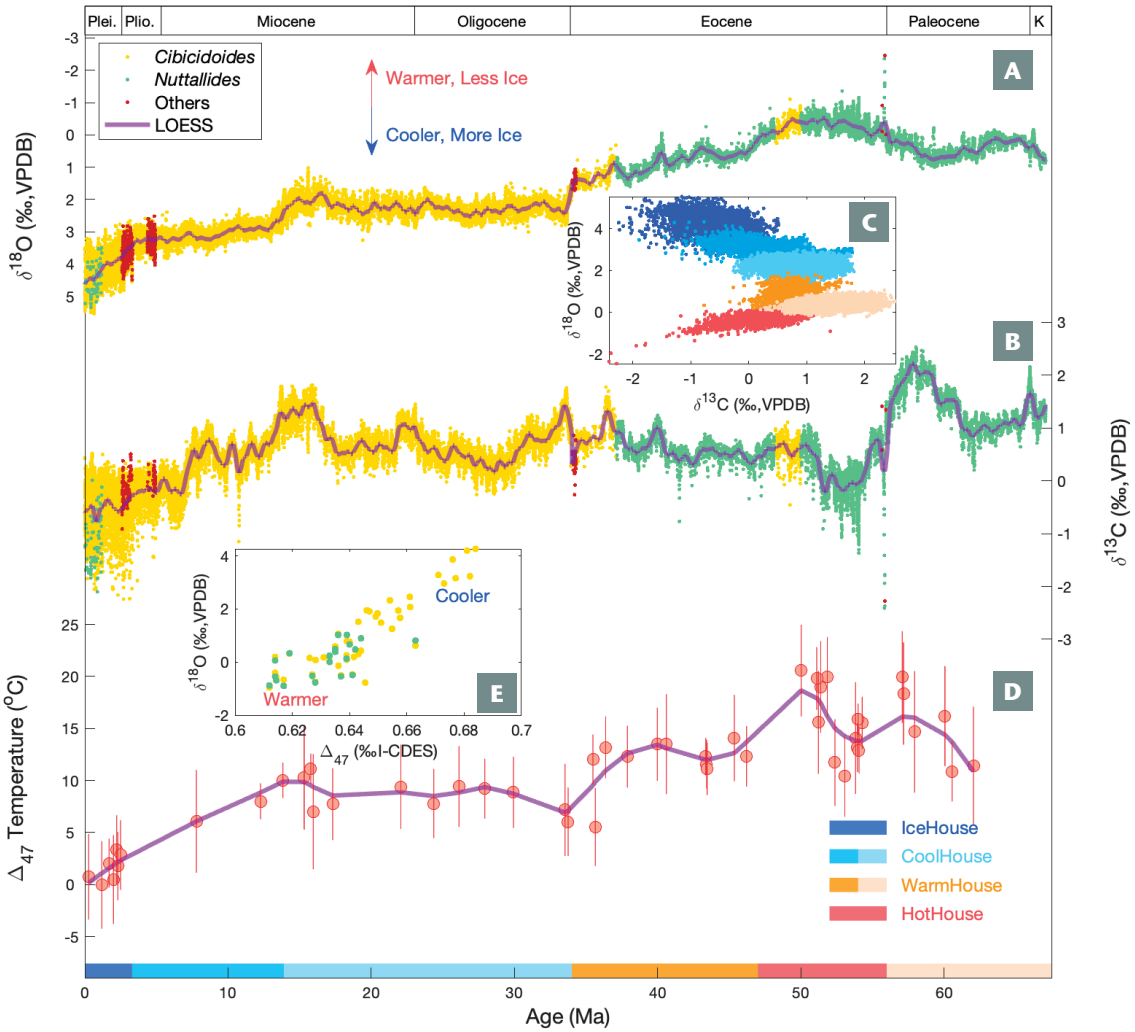

Figure 1 Cenozoic climate record based on $\delta^{18}O$, $\delta^{13}C$, and Δ_{47} of benthic foraminifera. (**A, B**) The CENOGRID composite $\delta^{18}O$ and $\delta^{13}C$ record (reported against the Vienna Pee Dee Belemnite standard) of deep ocean dissolved inorganic carbon (DIC) pool. Symbols represent different foraminifera genera, and species-specific offsets in $\delta^{18}O$ and $\delta^{13}C$ were applied to make the composite (Westerhold et al. 2020). The purple curve shows a 1-million-year LOESS smoothing of the data. (**C**) Cross plot of $\delta^{18}O$ and $\delta^{13}C$ in the CENOGRID record. Different colors represent Earth's different climate states during the Cenozoic (marked at the bottom) identified in Westerhold et al. (2020). (**D**) Cenozoic deep ocean temperature reconstructed from Δ_{47} (reported against the InterCarb-Carbon Dioxide Equilibrium Scale) of benthic foraminifera (Meckler et al. 2022). The circles with error bars show the Δ_{47}-derived temperatures and 95% confidence intervals as originally reported, and the purple line is a LOESS smoothing of the data. (**E**) Cross plot of foraminifera $\delta^{18}O$ and Δ_{47} over the Cenozoic showing the overall agreement of the two climate proxies (Meckler et al. 2022). Symbols represent different foraminifera genera as in (**A**) and (**B**).

VITAL EFFECTS: DISEQUILIBRIUM IN BIOGENIC CARBONATES

The link between measured isotopic changes and inferred environmental signals is based on principles of equilibrium fractionation. However, all biological processes, including those that make $CaCO_3$ minerals (i.e., biomineralization), involve disequilibrium. Deviations from isotopic equilibrium are called "kinetic isotope effects," while disequilibrium associated with biogenic carbonates are referred to as "vital effects" (Urey et al. 1951). When using carbonates as proxies for paleoenvironment, the hope is that these effects are either minimal or systematic enough to allow for reliable corrections to be made.

The magnitudes and patterns of vital effects have been characterized for various calcifying organisms, revealing similarities and differences that offer clues to their origin. In biogenic carbonates, more extreme deviations from equilibrium almost always result in lower (more negative) $\delta^{18}O$ and $\delta^{13}C$ values (Fig. 2A, 2B). If photosynthesis is involved, the $\delta^{13}C$ of some biogenic $CaCO_3$ can be elevated above equilibrium values, while the $\delta^{18}O$ values are sub-equilibrium, with the exception of some coccolithophores (Fig. 2B). Interestingly, a ubiquitous phenomenon in spatially sampled biominerals is that $\delta^{18}O$ and $\delta^{13}C$ are linearly correlated, even in the absence of significant environmental changes, which suggests a common causal mechanism (Fig. 2A, 2B; McConnaughey 1989a; Adkins et al. 2003; Chen et al. 2018). Meanwhile, the magnitude of the observed vital effects in some organisms can be as large as the benthic $\delta^{18}O$ and $\delta^{13}C$ variations through the entire Cenozoic (Fig. 1C). Such variability in stable isotopic composition is difficult to explain by environmental changes alone.

Some organisms, by contrast, exhibit minimal or constant deviations from isotope equilibrium, making them more attractive targets for paleoclimate reconstructions. For example, although depleted from equilibrium, the $\delta^{18}O$ of different foraminifera species generally show the same temperature sensitivity as inorganic $CaCO_3$, making species-specific offset corrections an effective way to remove the vital effects (Fig. 2C; Shackleton et al. 1984; Marchitto et al. 2014). A similar observation can be made for the clumped isotope thermometer, where the Δ_{47}–

temperature sensitivities of different organisms are similar to inorganic $CaCO_3$ (Fig. 2D; Ghosh et al. 2006; Meinicke et al. 2020). However, significant scatter exists in the empirical calibrations that limit the accuracy and precision of this thermometer in some cases (Fig. 2D).

Species-specific empirical calibrations in paleoclimate reconstruction are justified because they are effective at removing vital effects from paleoclimate records (Westerhold et al. 2020; Meckler et al. 2022). The downside of treating vital effects as a nuisance is that it draws attention away from some important research avenues: What causes the linear $\delta^{18}O$–$\delta^{13}C$ correlations (Fig. 2)? What drives $\delta^{18}O$ and $\delta^{13}C$ offsets between organisms? Why are some organisms more reliable recorders of their environment than others? Are species-specific offsets related to certain environmental conditions, and could those have changed through geologic time? The last question is particularly relevant for the early Cenozoic climate record, as a significant portion of the data come from an extinct *Nuttallides* species (Fig. 1). The accuracy of our interpretation of the biogenic carbonate archive critically depends on a better mechanistic understanding of these vital effects.

INORGANIC CARBONATES: A USEFUL REFERENCE FRAME

Evaluating vital effects requires a reference frame for equilibrium and non-equilibrium (kinetic) fractionation processes. For decades, researchers have grown carbonate minerals in the laboratory under controlled conditions to establish such a benchmark. These efforts showed, among other things, that stable isotope partitioning between carbonates and water depends on whether the crystals grow slowly, under near-equilibrium conditions, or rapidly, under far-from-equilibrium conditions. Under near-equilibrium conditions, isotope partitioning depends on temperature and is independent of the reaction mechanisms and pathways of crystal growth, allowing straightforward interpretations of equilibrium stable isotope values. Such conditions, however, are difficult to achieve in experiments and are the exception more than the rule in nature (Coplen 2007; Daëron et al. 2019).

The recognition that even laboratory-grown, inorganic carbonates precipitate out of isotopic equilibrium has prompted efforts to determine how the different reactions that form carbonate minerals influence their isotopic compositions. Consider, for example, carbonate growth from a CO_2-fed solution (Fig. 3A), which may be similar to some calcifying organisms. The incoming CO_2 reacts with H_2O and OH^- to form HCO_3^- and CO_3^{2-}, which are the anion "building blocks" of the $CaCO_3$ mineral. The stable isotope composition of these building blocks depends not only on the isotopic composition of the various reactants (CO_2, H_2O, and OH^-) but also on the tendency of isotopically light molecules of these compounds to react faster than their heavier counterparts, forming light isotope-enriched HCO_3^- and CO_3^{2-}. The quantity needed to describe the degree of light isotope enrichment in the resultant dissolved species is the "kinetic fractionation factor," which is equal to the ratio of isotope-specific (i.e., mass-dependent) rate constants for a particular reaction. Isotopes are additionally fractionated as these building blocks transfer to and from a mineral's surfaces, and again, there are kinetic fractionation factors attending these reactions. The kinetic isotope effects associated with the formation of HCO_3^- and CO_3^{2-} and their attachment to mineral surfaces tend to manifest most strongly at high-pH conditions, when the hydration/hydroxylation and mineral growth reactions are less reversible.

Characterizing how each reaction step contributes to the resulting isotopic composition of $CaCO_3$ is complicated, but significant progress has been made using a variety of approaches. For instance, to isolate the crystal growth

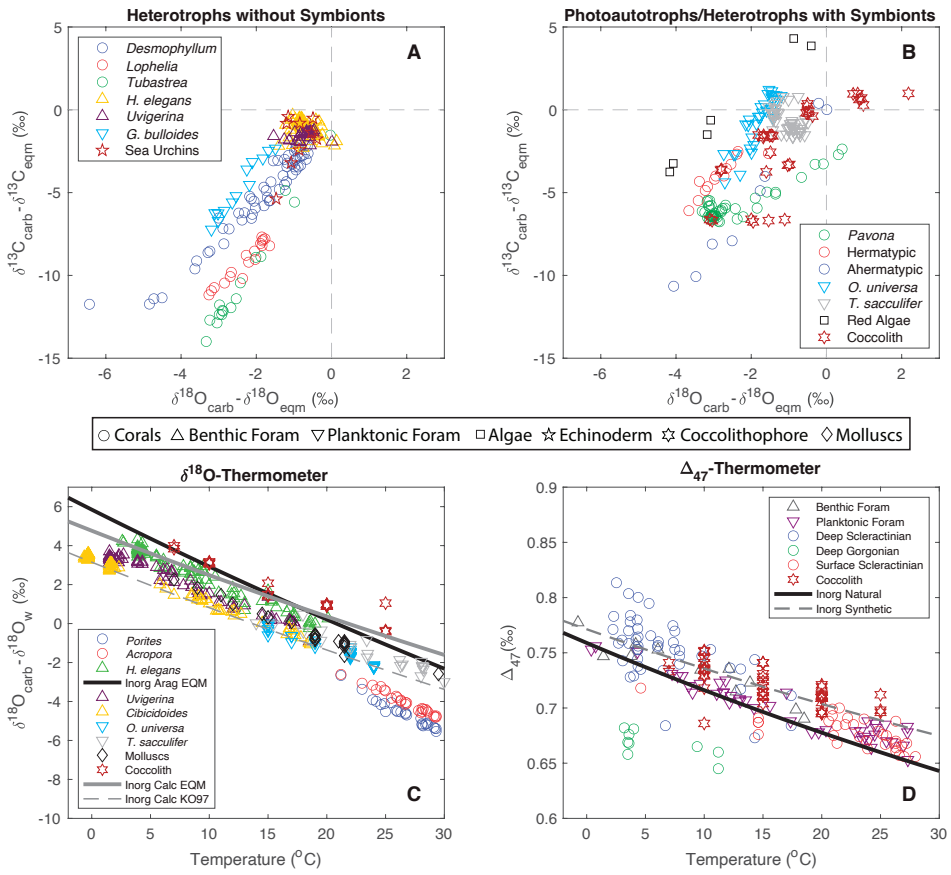

Figure 2 Compilation of $\delta^{18}O$, $\delta^{13}C$ and Δ_{47} determinations in biogenic carbonates that demonstrate vital effects (McConnaughey 1989a; Chen et al. 2018; Bergmann and Boekelheide 2021 and references therein). Different types of organisms are distinguished by symbol shape. (**A**) Correlations between $\delta^{18}O$ and $\delta^{13}C$ in heterotrophic calcifying organisms without photosymbionts. Data are plotted as deviations from estimated isotopic equilibrium based on temperature, $\delta^{18}O$ of seawater, and $\delta^{13}C$ of DIC. (**B**) Same as (**A**) but for photosynthetic calcifying organisms or organisms with photosymbionts. (**C**) $\delta^{18}O$–temperature calibrations for different calcifying organisms. The *y*-axis marks the difference between $\delta^{18}O$ of the carbonate mineral (VPDB) and seawater (VSMOW). The solid lines mark the likely equilibrium reference frame estimated from slow-growing natural calcite (gray line, Coplen 2007; Daëron et al. 2019) and synthetic aragonite (black line, Wang et al. 2013). The dashed line marks the commonly used inorganic calcite reference frame (Kim and O'Neil 1997) that is isotopically lighter than true equilibrium. (**D**) Δ_{47}–temperature calibrations for different calcifying organisms. The solid and dashed lines show calibrations from natural and synthetic inorganic carbonates, respectively (Daëron et al. 2019; Meinicke et al. 2020 and references therein).

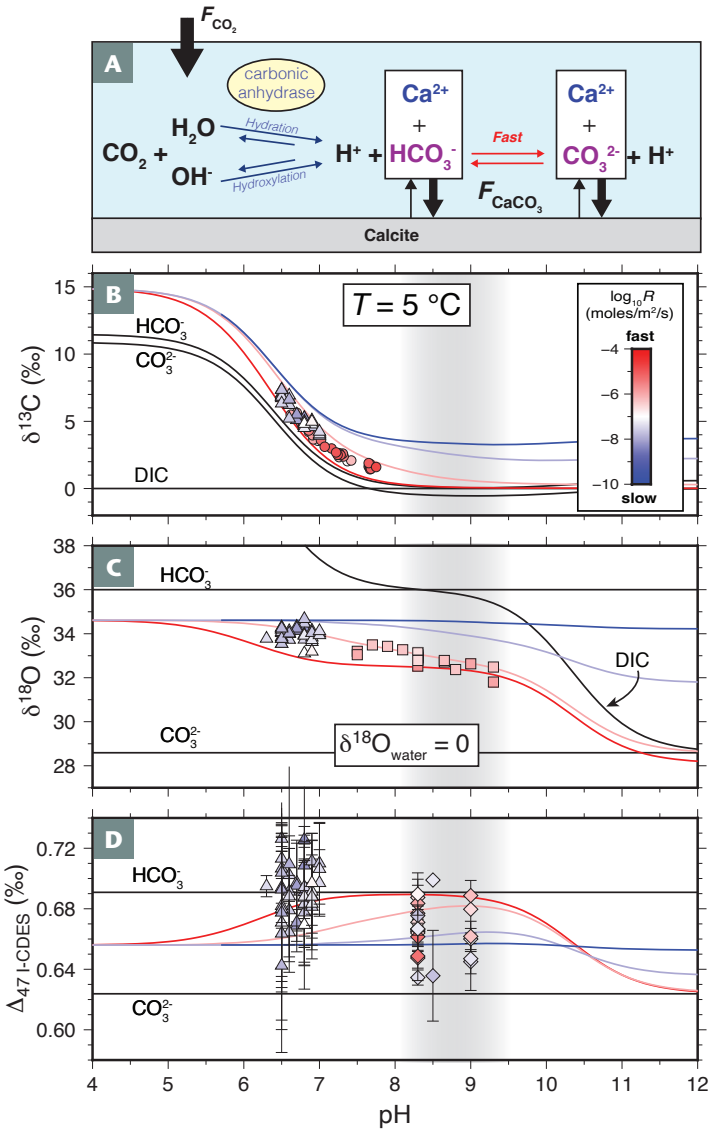

Figure 3 Process-based modeling of inorganic calcite precipitation experiments (normalized to 5 °C) in which the dissolved inorganic carbon (DIC) species were likely to have been equilibrated during calcite growth. (**A**) In experiments at constant pH, the enzyme carbonic anhydrase can be used to rapidly equilibrate CO_2 with HCO_3^-, thereby isolating kinetic isotope effects attending the crystal growth reactions (black arrows). (**B–D**) Outputs from an ion-by-ion model (curves) capture the pH- and growth rate-dependence, or lack thereof in the case of Δ_{47}, exhibited by the data (symbols represent different experimental studies). The gray shaded area shows the range of observed and estimated pH at the site of calcification in corals and foraminifera. Modified from Watkins and Devriendt (2022).

reaction (black arrows in Fig. 3A), the enzyme carbonic anhydrase has been used to facilitate isotopic exchange between CO_2 and H_2O (Uchikawa and Zeebe 2012) so that the isotopic compositions of the anion building blocks are equilibrated and therefore known. Under these special conditions, the kinetic fractionation factors between calcite and HCO_3^-/CO_3^{2-} can be determined by comparing model-derived curves to experimental determinations (Fig. 3B–3D; Watkins and Devriendt 2022 and references therein). Meanwhile, the kinetic fractionation factors of the hydration and hydroxylation reactions (blue arrows in Fig. 3A) have been adequately determined only recently through carefully designed laboratory experiments (Yumol et al. 2020) and field studies (Christensen et al. 2021) that minimize the effects of the reverse reactions. A key outcome of these efforts is a model of the equilibrium and kinetic isotope fractionations within the inorganic DIC–$CaCO_3$–H_2O system, which constitutes a powerful tool in the quest to demystify vital effects and more accurately decipher the carbonate archive.

BIOMINERALIZATION: CONTROLLED DISEQUILIBRIUM BY CALCIFYING ORGANISMS

The reference frame built from inorganic experiments requires at least two conditions to achieve equilibrium fractionation in the carbonate mineral: (1) sufficient time for isotope equilibration between DIC and water (seconds to minutes for $\delta^{13}C$, hours to days for $\delta^{18}O$ in alkaline conditions; McConnaughey 1989b; Uchikawa and Zeebe 2012); (2) sufficiently slow mineral growth to allow equilibration at the mineral–fluid interface. Neither condition is likely to be met for relatively fast-growing biogenic carbonates. Marine calcifying organisms can additionally deviate from equilibrium with seawater by modifying the chemical and isotopic composition of the fluid from which the $CaCO_3$ minerals grow, with further complications from involvement of organic carbon through photosynthesis/respiration. To understand the effects each factor imposes upon the $CaCO_3$ mineral, a comprehensive biomineralization model is needed that takes into account both the biological calcification and physicochemical isotope fractionation processes.

After decades of in-depth study from biophysical, morphological, and geochemical perspectives, an integrated model for $CaCO_3$ biomineralization has been developed that is applicable to a wide variety of calcifying organisms (Fig. 4A; Gilbert et al. 2022 and references therein). The key features of this model include: (1) Calcification takes place in a space in the organism (either intercellular or extracellular) from fluid that is derived from but differs from ambient seawater. (2) This space contains calcifying fluid (CF) from which $CaCO_3$ precipitates, with the chemical composition of the CF modified by the organism, tending to increase its pH as well as Ca^{2+} and DIC concentrations to facilitate growth of the biomineral. (3) Ions used for calcification come from active pumping by ion channels on the membranes around the CF and/or paracellular seawater transport. An additional source of carbon is by diffusion of neutral CO_2 molecules through membranes that can be influenced by metabolic processes. (4) $CaCO_3$ biomineralization occurs through two major pathways, particle attachment (PA) and ion attachment (IA). PA takes place through rapid formation of amorphous calcium carbonate (ACC) nanoparticles in the highly saturated CF, which are the building blocks and precursors to the final crystalline mineral. In contrast, IA is similar to inorganic precipitation that is typically much slower than PA, and acts to fill the space left unfilled by the ACC particles.

The key question that presents itself is: How do these processes act to mechanistically explain the stable isotope deviations from equilibrium described above? The CF essentially operates as a CO_2-fed solution, similar to the inorganic calcite experiments shown in Figure 3. However, it includes an "alkalinity pump" where Ca^{2+} (and/or other cations) enter the solution in exchange for H^+ ions. This active removal of H^+ can counteract the acidifying effects of CO_2, leading to an increase in pH (de Nooijer et al. 2009; Venn et al. 2011). This pH increase is crucial, as it significantly impacts the stable isotope composition of the final mineral in several ways: (1) It slows down isotopic equilibration between DIC and water, promoting light isotope enrichment in HCO_3^- and CO_3^{2-}; (2) It leads to greater supersaturation, promoting faster crystal growth that can preserve larger kinetic isotope effects; (3) It increases the

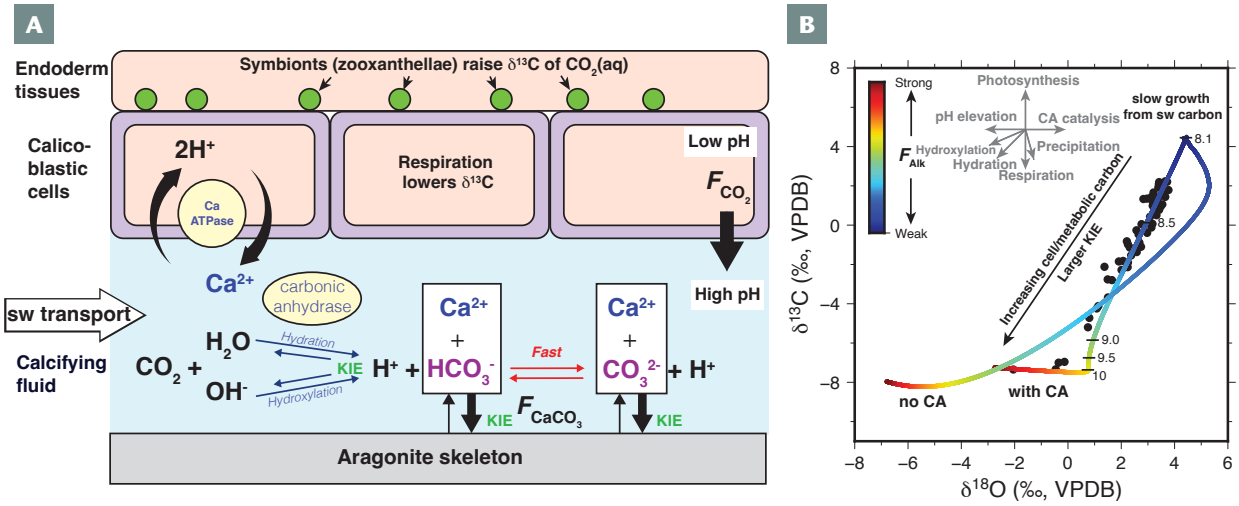

Figure 4 (**A**) Process-based model for calcification, adapted to corals as a model organism, that takes into account lessons from inorganic experiments (see similarities to Fig. 3A), as well as the influence of symbionts and respiration on $\delta^{13}C$ of CO_2. The "sw transport" component includes seawater (sw) transport via vacuolization as well as seawater infiltration into the porous skeleton. (**B**) A quantitative representation of the model, with inclusion of biological factors such as internal pH elevation and catalysis by carbonic anhydrase, can explain the slope and range of $\delta^{13}C$–$\delta^{18}O$ co-variations observed in an individual deep-sea coral (black dots). The gray arrows show how different processes influence $\delta^{13}C$ and $\delta^{18}O$ of the internal DIC pool during biomineralization. Abbreviations: CF = calcifying fluid; CA = carbonic anhydrase; KIE = kinetic isotope effect. Modified from Chen et al (2018).

concentration gradient of CO_2(aq) between the calcifying fluid and cell cytoplasm, and shifts the carbon source from predominantly seawater DIC to metabolic carbon with much lower $\delta^{13}C$ (Fig. 4B; McConnaughey 1989a; Adkins et al. 2003; Chen et al. 2018).

A quantitative version of these concepts shows promise for demystifying vital effects. Focusing on deep-sea corals, Chen et al. (2018) wrote a set of equations that includes cross-membrane CO_2 transport, seawater infiltration, alkalinity pumping, and the physicochemical rules of DIC–H_2O and DIC–$CaCO_3$ isotope exchange reactions. Numerical solutions to these equations can reproduce the $\delta^{18}O$–$\delta^{13}C$ correlations in coral individuals (Fig. 4B), and in so doing, reveal probable values of the pH of the CF and strength of the alkalinity pump. A key insight is that the $\delta^{18}O$–$\delta^{13}C$ slope is sensitive to the activity of carbonic anhydrase in the CF as well as the $\delta^{13}C$ and residence time of cross-membrane CO_2(aq), a possible explanation for why different calcifying organisms exhibit different slopes (Fig. 2A, 2B). For example, photosynthesis incorporates ^{13}C-depleted carbon into organic matter, which elevates the $\delta^{13}C$ of cross-membrane CO_2(aq) and decreases the $\delta^{18}O$–$\delta^{13}C$ slope (McConnaughey 1989a), while incorporation of respiratory CO_2 can cause depletions in both $\delta^{13}C$ and $\delta^{18}O$ of the biomineral (Erez 1978). Meanwhile, the residence time of CO_2(aq) and carbonic anhydrase activity in the CF can both influence the amount of kinetic isotope effects preserved in the $CaCO_3$ mineral and, therefore, $\delta^{18}O$–$\delta^{13}C$ slopes (Chen et al. 2018; Chauhan and Rickaby 2024).

Given the similar biomineralization processes observed in different calcifying organisms, the coral-based quantitative model can be adapted to other calcifying organisms by adjusting key parameters, such as the strength of alkalinity pumps and the seawater turnover rate, which helps to reveal and quantify the key biological processes that cause vital effects. An open question relevant for foraminifera-based paleoclimate records is whether offsets in the absolute $\delta^{18}O$ and $\delta^{13}C$ values among different species are caused by organism-specific pH up-regulation or growth-rate dependent kinetic fractionation at the mineral–fluid interface (or both), and whether these effects are themselves dependent on environmental conditions such as seawater pH. Another frontier regards the growth mechanisms through PA versus IA in different organisms, and how these affect the isotopic composition of $CaCO_3$. It will also be interesting to see how such models perform for clumped isotopes and whether they can account for the vital effects in various organisms.

OUTLOOK

Quantitative paleoclimate reconstructions were born with the first measurements of $\delta^{18}O$ on carbonate minerals around 75 years ago. Improved sampling and measurement techniques, along with the development of new methods such as clumped isotope thermometry, continue to refine our knowledge of climate change, from seasonal to Phanerozoic timescales. The records are derived largely from the remains of once-living organisms, and so-called "vital effects" have long complicated the interpretation of stable isotope data. Although empirical corrections have been applied with great success, there is much to be gained in the coming years from simplified but useful process-based models. Understanding how organisms respond to environmental changes will lead to exciting new discoveries into their adaptive strategies as well as more accurate models for past, present, and future climate scenarios.

ACKNOWLEDGMENTS

We thank Michael Bender for sharing his perspective on early drafts. We gratefully acknowledge contributions from Don DePaolo, an anonymous reviewer, and the editors of the issue, including principal editor Tom Sisson during the review process, all of which improved the quality and clarity of the manuscript considerably. SC acknowledges financial support from National Key R&D Program of China 2023YFF0806100 and NSFC grant 42103081. JW was supported by NSF-CAREER Grant no. EAR1749183.

REFERENCES

Adkins JF, Boyle EA, Curry WB, Lutringer A (2003) Stable isotopes in deep-sea corals and a new mechanism for "vital effects". Geochimica et Cosmochimica Acta 67: 1129-1143, doi: 10.1016/S0016-7037(02)01203-6

Bergmann KD, Boekelheide N (2021) A shift from equilibrium: analysis of isotopic variability across modern biomineralizing organisms (OSF, 2021), doi: 10.17605/OSF.IO/RVC58

Chauhan N, Rickaby REM (2024) Size-dependent dynamics of the internal carbon pool drive isotopic vital effects in calcifying phytoplankton. Geochimica et Cosmochimica Acta 373: 35-51, doi: 10.1016/j.gca.2023.10.005

Chen S, Gagnon AC, Adkins JF (2018) Carbonic anhydrase, coral calcification and a new model of stable isotope vital effects. Geochimica et Cosmochimica Acta 236: 179-197, doi: 10.1016/j.gca.2018.02.035

Christensen JN and 7 coauthors (2021) Isotopic fractionation accompanying CO_2 hydroxylation and carbonate precipitation from high pH waters at The Cedars, California, USA. Geochimica et Cosmochimica Acta 301: 91-115, doi: 10.1016/j.gca.2021.02.019

Coplen TB (2007) Calibration of the calcite–water oxygen-isotope geothermometer at Devils Hole, Nevada, a natural laboratory. Geochimica et Cosmochimica Acta 71: 3948-3957, doi: 10.1016/j.gca.2007.05.028

Daëron M and 7 coauthors (2019) Most Earth-surface calcites precipitate out of isotopic equilibrium. Nature Communications 10: 429, doi: 10.1038/s41467-019-08336-5

de Nooijer LJ, Toyofuku T, Kitazato H (2009) Foraminifera promote calcification by elevating their intracellular pH. Proceedings of the National Academy of Sciences 106: 15374-15378, doi: 10.1073/pnas.0904306106

Emiliani C (1955) Pleistocene temperatures. The Journal of Geology 63: 538-578, doi: 10.1086/626295

Erez J (1978) Vital effect on stable-isotope composition seen in foraminifera and coral skeletons. Nature 273: 199-202, doi: 10.1038/273199a0

Fairbanks RG, Dodge RE (1979) Annual periodicity of the $^{18}O/^{16}O$ and $^{13}C/^{12}C$ ratios in the coral *Montastrea annularis*. Geochimica et Cosmochimica Acta 43: 1009-1020, doi: 10.1016/0016-7037(79)90090-5

Ghosh P and 7 coauthors (2006) ^{13}C–^{18}O bonds in carbonate minerals: A new kind of paleothermometer. Geochimica et Cosmochimica Acta 70: 1439-1456, doi: 10.1016/j.gca.2005.11.014

Gilbert PUPA and 12 coauthors (2022) Biomineralization: integrating mechanism and evolutionary history. Science Advances 8: eabl9653, doi: 10.1126/sciadv.abl9653

Kim ST, O'Neil JR (1997) Equilibrium and nonequilibrium oxygen isotope effects in synthetic carbonates. Geochimica et Cosmochimica Acta 61: 3461-3475, doi: 10.1016/S0016-7037(97)00169-5

Kirtland Turner S (2014) Pliocene switch in orbital-scale carbon cycle/climate dynamics. Paleoceanography 29: 1256-1266, doi: 10.1002/2014PA002651

Marchitto TM and 5 coauthors (2014) Improved oxygen isotope temperature calibrations for cosmopolitan benthic foraminifera. Geochimica et Cosmochimica Acta 130: 1-11, doi: 10.1016/j.gca.2013.12.034

McConnaughey T (1989a) ^{13}C and ^{18}O isotopic disequilibrium in biological carbonates: I. Patterns. Geochimica et Cosmochimica Acta 53: 151-162, doi: 10.1016/0016-7037(89)90282-2

McConnaughey T (1989b) ^{13}C and ^{18}O isotopic disequilibrium in biological carbonates: II. In vitro simulation of kinetic isotope effects. Geochimica et Cosmochimica Acta 53: 163-171, doi: 10.1016/0016-7037(89)90283-4

Meckler AN and 10 coauthors (2022) Cenozoic evolution of deep ocean temperature from clumped isotope thermometry. Science 377: 86-90, doi: 10.1126/science.abk0604

Meinicke N and 6 coauthors (2020) A robust calibration of the clumped isotopes to temperature relationship for foraminifers. Geochimica et Cosmochimica Acta 270: 160-183, doi: 10.1016/j.gca.2019.11.022

Saenger C and 5 coauthors (2012) Carbonate clumped isotope variability in shallow water corals: temperature dependence and growth-related vital effects. Geochimica et Cosmochimica Acta 99: 224-242, doi: 10.1016/j.gca.2012.09.035

Shackleton NJ, Hall MA, Boersma A (1984) Oxygen and carbon isotope data from Leg 74 foraminifers. In: Moore TC, Rabinowitz PD Al PD (eds) Initial Reports of the Deep Sea Drilling Project 74, U.S. Government Printing Office, Washington DC, pp 599-612, doi: 10.2973/dsdp.proc.74.117.1984

Uchikawa J, Zeebe RE (2012) The effect of carbonic anhydrase on the kinetics and equilibrium of the oxygen isotope exchange in the CO_2–H_2O system: Implications for $\delta^{18}O$ vital effects in biogenic carbonates. Geochimica et Cosmochimica Acta 95: 15-34, doi: 10.1016/j.gca.2012.07.022

Urey HC, Lowenstam HA, Epstein S, McKinney CR (1951) Measurement of paleotemperatures and temperatures of the Upper Cretaceous of England, Denmark, and the southeastern United States. Geological Society of America Bulletin 62: 399-416, doi: 10.1130/0016-7606(1951)62[399:MOPATO]2.0.CO;2

Venn A, Tambutté E, Holcomb M, Allemand D, Tambutté S (2011) Live Tissue Imaging Shows Reef Corals Elevate pH under Their Calcifying Tissue Relative to Seawater. PLOS ONE 6: e20013, doi: 10.1371/journal.pone.0020013

Wang Z, Gaetani G, Liu C, Cohen A (2013) Oxygen isotope fractionation between aragonite and seawater: developing a novel kinetic oxygen isotope fractionation model. Geochimica et Cosmochimica Acta 117: 232-251, doi: 10.1016/j.gca.2013.04.022

Watkins JM, Devriendt LS (2022) A combined model for kinetic clumped isotope effects in the $CaCO_3$-DIC-H_2O system. Geochemistry, Geophysics, Geosystems 23: e2021GC010200, doi: 10.1029/2021GC010200

Westerhold T and 10 coauthors (2020) An astronomically dated record of Earth's climate and its predictability over the last 66 million years. Science 369: 1383-1387, 10.1126/science.aba6853

Yumol LM, Uchikawa J, Zeebe RE (2020) Kinetic isotope effects during CO_2 hydration: Experimental results for carbon and oxygen fractionation. Geochimica et Cosmochimica Acta 279: 189-203, doi: 10.1016/j.gca.2020.03.008

Zachos J, Pagani M, Sloan L, Thomas E, Billups K (2001) Trends, rhythms, and aberrations in global climate 65 Ma to present. Science 292: 686-693, doi: 10.1126/science.1059412. ■